2-D Magnetohydrostatic Configurations Leading to Flares or Quiescent Filament Eruptions

C.-H. An*, S. T. Suess, and R. L. Moore
NASA/Marshall Space Flight Center
ES-52, Space Science Laboratory
Huntsville, AL 35812

*NRC research associate

ABSTRACT

To investigate the cause of flares and quiescent filament eruptions we have studied the quasi-static evolution of a magnetohydrostatic (MHS) model. The results lead us to propose that: (1) The sudden disruption of an active-region filament field configuration and the accompanying flare result from the lack of a neighboring equilibrium state as magnetic shear is increased above a critical value. (2) A quiescent filament eruption is due to an ideal MHD kink instability of a highly twisted detached flux tube formed by the increase of plasma current flowing along the length of the filament.

For the study we have developed a numerical solution to the 2-D MHS equation for the self-consistent equilibrium of a filament and overlying coronal magnetic field. Because the initial arcade (potential field) configuration is completely stable to global MHD modes, the field must evolve from a simple arcade to a geometry with sheared field or with a detached helically twisted tube along the axis of the filament before reaching an unstable state corresponding to the onset of a flare or an eruption. The change can be made by increasing the axial and/or the poloidal current. Increase of the poloidal current causes increase of magnetic shear. As shear increases past a critical point, there is a discontinuous topological change in the equilibrium configuration. We propose that the lack of a neighboring equilibrium triggers a flare. Increase of the axial current results in a detached tube with enough helical twist to be unstable to ideal MHD kink modes. We propose that this is the condition for the eruption of a quiescent filament.

I. INTRODUCTION

Solar filaments, whether in active regions or quiet regions, sometimes violently disrupt. An active-region filament resides along a neutral line between regions of opposite polarity magnetic field, where the field is strongly sheared, and where the field magnitude is 100-1000 G. Active-region filament eruptions along with flares are most likely to occur when and where the field shear is strongest, i.e. when and where the field at the neutral line becomes nearly aligned with the neutral line (Hagyard, et al., 1984; Hagyard and Rabin, 1986). In these events, the active region filament eruption is clearly an integral part of the accompanying flare (Moore, et al., 1984; Moore, et al., 1986). A quiescent filament, i.e., a filament in a quiet region, also resides in the magnetic field above a magnetic neutral line, but differs from an active region filament in that the magnetic field is less sheared and no stronger than a few tens of gauss (Tandberg-Hanssen, 1974). Some quiescent-filament eruptions are not accompanied by appreciable flare brightening in the chromosphere (Svestka, 1976). Erupting quiescent filaments often appear to have an overall helical twist, with several complete turns from one end to the other (Tandberg-Hanssen, 1974; Priest, 1984). In contrast, erupting active-region filaments usually do not show obvious multiple turns or twist; rather, they often appear to have an overall twist of one turn or less (Roy and Tang, 1975; Moore, et al., 1986). These differences suggest that the mechanism for eruption of quiescent filaments may be different from that of active region filament.

Various theoretical models have been proposed to explain filament eruptions. Sakurai (1976) showed that the eruption can occur due to an ideal MHD kink instability as twist increases above a certain critical value. Noting that all eruptive filaments and coronal loops have foot points anchored in the photosphere, other authors have studied the effect of line-tying on the MHD stability of a loop (Raadu, 1972; Hood and Priest, 1979; An, 1982, 1984; Einaudi and Van Hoven, 1981), demonstrating its stabilizing effect. Other authors have studied the quasi-static evolution of force free magnetic fields in connection with the onset of filament eruptions and flares (Barnes and Sturrock, 1972; Low, 1977; Jockers, 1976, 1978; Heyvaerts, et al., 1982; Birn, et al., 1978; Priest and Milne, 1980; Aly, 1985; Yang, et al., 1985). In these studies, the magnetic field geometry is considered to be invariant along the length of the filament channel. The force free equation then becomes a two dimensional problem that can be solved by specifying the component of the magnetic field along the filament as a function of a vector potential that only has one component-also along the filament. Force-free models invariably show that as the magnetic field along the filament (closely related to magnetic shear) increases above a critical value, no solution exists, or there is a discontinuity in the topology of the solution. Here, these conditions will be refered to as the lack of a neighboring equilibrium- a situation which has been regarded as the onset of a filament eruption and flare.

Even though extensive studies have been done to understand why filaments erupt, the observed differences between quiescent filaments and active-region filaments have not been taken into account. Is the MHD kink instability the mechanism for active-region filament eruptions with flares, as well as for quiescent-filament eruptions? Since an active-region filament resides in a magnetic field that is nearly parallel to the neutral line, then if this field becomes detached from the photosphere to form a long, helical flux tube, the overall twist could well be small enough as to preclude the MHD kink instability as the mechanism for an active region filament eruption. On the other hand, it is unlikely that the lack of a neighboring equilibrium is the mechanism for a quiescent-filament eruption with high field twist. In a quiescent filament with smaller field strength than in an active-region filament, an initial arcade field can evolve into one with a detached flux tube with high twist from less axial current than that for the same amount of helical twist in an active-region filament. Under conditions that will be defined below, increasing the axial current can instead result in the lack of a neighboring equilibrium. However, as we will show, it is probable that the field configuration of a quiescent filament becomes kink unstable due to a high twist before the lack of a neighboring equilibrium is reached.

Therefore, in this study, we propose separate mechanisms for the two eruptive phenomena, based on the observations that active regions have highly sheared magnetic structures while quiet regions have less magnetic shear: quiescent filaments erupt due

to ideal MHD kink instability as the initial arcade magnetic structure evolves to have a detached flux tube with high magnetic twist floating above the neutral line, whereas active region flares occur due to the lack of a neighboring equilibrium as magnetic shear increases over a critical value. For this study, we construct magnetohydrostatic (MHS) configurations and model the quasi-static evolution of the configuration by changing the magnitude of axial and poloidal currents. Most theoretical work for quasi-static evolution has concentrated on the evolution of force free fields with field geometry not representative of solar filaments and have not taken into account the stability of the magnetic fields during the evolution. The concept of the quasi-static evolution is valid only when the equilibrium is stable during the evolution. Our study of quasi-static evolution differs from the previous studies on the following aspects. We have built realistic MHS equilibria with geometry similar to that of the magnetic field in and around real filaments, geometry based on observations (Kawaguchi, 1967; Saito and Tandberg-Hanssen, 1973; Waldmeier, 1970) showing quiescent filaments with sheared fields in the low interiors of coronal streamers the outer parts of which exhibit a coronal magnetic field with much less shear. Active-region filaments are also observed (Hagyard, Moore, and Emslie, 1984) to have highly sheared fields along the neutral line, and to be surrounded by less sheared coronal magnetic fields. We also apply a one-dimensional ideal MHD stability criterion to each equilibrium to test its stability.

We present sequences of MHS equilibria which show field configurations with increasing field twist or increasing magnetic shear. The results are used to explain filament eruptions. However, we emphasize that even though we have filaments in mind for the study, we do not consider the detailed process of their formation, but focus on magnetohydrostatic aspects leading to their eruption. Our model represents the entire "filament channel", i.e., the entire closed bipolar magnetic field configuration in which the filament is embedded. To gain insight into why and how filaments erupt, we model the overall MHS configuration and how it might evolve to lose its equilibrium.

II. MAGNETOHYDROSTATIC MODEL FOR FILAMENT REGIONS

(a) Model Description and Governing Equations.

Our phenomenological description of filament magnetic fields suggests a "standard empirical model" having two basic features: (i) magnetic shear concentrated near the photospheric neutral line so that the field within the filament above the neutral line is predominantly directed along the filament, and (ii) helical twist in this predominantly axial field in and around the filament. Seeking the simplest physical case as well as a model that is mathematically tractable, we assume an isothermal plasma in a constant gravitational field. The configuration is shown schematically in Fig. 1. In this figure, gravity is in the negative z-direction, all variables are independent of the x-coordinate, and the magnetic neutral line is in the x-y plane and along the x-axis.

Any magnetic field that incorporates these symmetries can be written as the sum of the curl of the x-component of a vector potential, A, and the x-component of the field. That is:

$$\vec{B} = \nabla \times (A\,\vec{e}_x) + B_x\,\vec{e}_x \tag{1}$$

The governing magnetostatic equilibrium equations are:

$$\nabla p = \frac{1}{c}\,\vec{j} \times \vec{B} - \rho g\,\vec{e}_z \tag{2}$$

$$\vec{j} = \frac{c}{4\pi}\,\nabla \times \vec{B} \tag{3}$$

$$p = R\,\rho\,T \tag{4}$$

where gaussian units are used, $\vec{j}$ is the current density, $-g\,\vec{e}_z$ is the gravitational acceleration, p is pressure, ρ is density, T is the temperature, R is the gas constant, and $\vec{e}_x$ is the unit vector in x-direction.

These equations can be reduced to a Poisson equation for the potential, A, which will be solved in a manner similar to that by Low (1977), we first make a change of variable from p(x,y) to Q, where Q is defined as

$$Q = p(x,y)e^{\lambda z}$$

$$\lambda z = \int_0^z \frac{g}{RT}\,dz = \frac{g}{RT}\,z \tag{5}$$

Making this change and taking the scalar product of (2) with the magnetic field allows us to show that

$$Q = Q(A)$$

That is, Q is a function of A alone. By taking the x-component of (2), we can also show that $\nabla A \times \nabla B_x = 0$ or, equivalently, that $B_x = B_x(A)$. Thus these two functions are constant on surfaces of constant A- a result which will be used in specifying the boundary conditions. With these two results, equation (3) can be re-written in the form:

$$\nabla^2 A + 4\pi \frac{dQ}{dA} e^{-\lambda z} + B_x \frac{dB_x}{dA} = 0 \ .$$

By defining

$$f(A) = 4\pi \frac{dQ}{dA}$$

we note that

$$P(y,z) = e^{-\lambda z}[P_o + \frac{1}{4\pi} \int_o^A f(A)dA] \qquad (6)$$

where p_o is the ambient plasma pressure at the base of the model, then we finally derive the desired equation

$$\nabla^2 A + f(A) e^{-\lambda z} + B_x \frac{dB_x}{dA} = 0 \qquad (7)$$

which will be solved for the "flux function" A. In (7) $B_x(A)$ and f(A) can be considered as "source functions". We note that the pressure remains unmodified by the presence of the magnetic field if f(A) = 0; so even though $B_x = 0$, any solution for which f(A) = 0 is, necessarily, a force free magnetic field solution.

Following the approach of Zweibel and Hundhausen (1982) in solving (7), we assume specific functional forms for the dependence of the two source functions on A. The selection of these functions will be motivated by our "standard empirical model" of the magnetic field configuration of a filament channel. That is, that shear is confined to the vicinity of the magnetic neutral line and the functions be smooth. We take two cases. First:

$$\begin{aligned} B_x(A) &= \gamma(A - A_c)^2 \quad \text{for} \quad A > A_c \\ &= 0 \qquad\qquad\ \ \text{for} \quad A_c > A > 0 \end{aligned} \tag{8}$$

and, second:

$$\begin{aligned} B_x(A) &= \gamma(A - A_c)^2 \quad \text{for} \quad 1 > A > A_c \\ &= \gamma(1 - A_c)^2 \quad \text{for} \quad A > 1 \\ &= 0 \qquad\qquad\ \ \text{for} \quad A_c > A > 0 \ . \end{aligned} \tag{9}$$

In both cases, we assume that

$$f(A) = \alpha^2 A.$$

In the above, A = 0 at y = ±D/2 and A = 1 at y = 0, on the lower boundary.

The choices for $B_x(A)$ are made with the motivation of producing axial field and hence shear only locally near the magnetic neutral line. The dependence on A in (8) and (9) insures that this is the case. The quadratic variation of B_x with A guarantees that it is a smooth function and is continuous across the boundary between the regions with and without B_x. There is no difference between the variations given in (8) and (9) if the maximum value of A lies on the lower boundary. However, as α is increased past a particular value, (α_p, determined by the value of γ), the location of the maximum in A moves above the lower boundary. The physical meaning of this can be seen more easily in terms of the magnetic field. For $\alpha < \alpha_p$, all magnetic field lines intersect the lower boundary. For $\alpha > \alpha_p$, some magnetic field lines are helices whose axes are parallel to the magnetic neutral line and who lie entirely above the x-y plane; these will be called "detached field lines". This development of a detached helical tube will be demonstrated (Fig.3).

It turns out that (8) leads to the absence of any equilibrium solutions for γ greater than a calculable critical value, γ_c, whereas (9) results in a jump to a non-neighboring equilibrium for $\gamma > \gamma_c$, and shows that the shear continues to increase as γ increases past γ_c. It is for this reason that the second choice for $B_x(A)$ in (9) is introduced. We believe there

is little physical significance in one choice resulting in a discontinuity in solution topology and the other choice resulting in no solutions for $\gamma > \gamma_c$ since, as we will show, the solutions at $\gamma > \gamma_c$ have much larger total energy than those of $\gamma < \gamma_c$ and hence are probably physically unattainable. Rather, reaching the critical value of γ seems to indicate the onset of dynamic non-equilibrium.

The physical significance of the choices for the source functions can be seen by computing the poloidal (y-z plane) and axial (along the x-axis) current systems produced by the source functions. These are:

$$\vec{j}_p = \frac{c}{4\pi} \frac{dB_x}{dA} \nabla A \times \vec{e}_x \tag{11}$$

$$j_x = \frac{c}{4\pi} [f(A)\, e^{-\lambda z} + B_x \frac{dB_x}{dA}] = - \frac{c}{4\pi} \nabla^2 A \tag{12}$$

As indicated in Figure 1, the magnitude of A_c determines how localized the poloidal current is around the x-axis.

The magnetic field lines depicted in Figure 1, which are a solution to (7) for a specific set of parameters and not merely a schematic, reflect the intent of our model to simulate the standard empirical model for a filament magnetic field. The figure shows a sheared magnetic field surrounded by non-sheared field, motivated by the observations of solar filaments with sheared field inside a coronal magnetic arcade with much less shear. A localized shear can only be described by functions like those in (8) or (9) - that are small for values of the potential

A smaller than some specified value, so these selections for the source function are representative of the current systems that exist on the sun. The plasma beta (the ratio of plasma pressure to magnetic pressure) in the model should also be representative of the corona in filament channels. β is less than 10^{-2} in active regions and less than 1 in quiet regions. In the model, β depends on the detailed form and amplitude of the source functions. Equation (8) gives smaller β values for high α than eq.(9) does, so this choice is used for modeling the evolution of quiescent filament channels under changing α.

For boundary conditions on A, we impose the following:

$$\begin{aligned} A &= \cos(\pi y/D) && \text{at } z = 0 \\ &= 0 && \text{at } z = \infty \\ &= 0 && \text{at } y = \pm D/2. \end{aligned}$$

These conditions require that the potential be periodic on the lower boundary and that no field lines cross the side-boundaries of the computing domain. The boundary condition at $z = \infty$ then insures that there be no source of magnetic flux except at the lower boundary. To cover the entire domain defined by these boundary conditions in the numerical solution to (7), we transform y-z space to y-w space by defining a new vertical coordinate, w, (Zweibel and Hundhausen, 1982) to be

$$w = e^{-\frac{\lambda}{2} z}.$$

The computational domain, then, become $0 \leq w \leq 1$ and $-D/2 \leq y \leq D/2$. To solve the MHS equilibrium equation (7) we use the Buneman Poisson solver (Buneman, 1969). This numerical method is extremely efficient for rectangular geometry and Dirichlet boundary conditions - even for our highly nonlinear source functions. For the ambient coronal plasma (Withbroe and Noyes, 1977), we adopt temperature $T = 2 \times 10^6 k$ and particle number density $n = 5 \times 10^9 k$ cm^{-3}, so β is about 0.001 for an active region with field strength about 200 gauss. For a quiet region with $T = 2 \times 10^6$, $n = 5 \times 10^8$ cm^{-3}, and field strength about 5 gauss, β is about 0.1. The magnitude of β near the neutral line increases as the equilibrium departs from a force free state by the increase of the longitudinal current.

(b) Definition of Field Twist

Since the concept of quasi-static evolution is physically valid only when each equilibrium of the sequence is stable, we have to test the stability. According to stability calculations of cylindrical geometry (Hood and Priest, 1980; Ray and Van Hoven, 1982; Migliuolo and Cargill, 1983), an arcade field configuration with all the field lines tied to the photosphere is ideal MHD stable. However, Hood and Priest (1980) show that the equilibrium can be unstable when the quasi-static evolution produces a detached flux tube above and parallel to the neutral line inside of the arcade. Thus, we have to check the stability for MHS solutions containing a detached flux tube. Bateman (1978) calculated the stability criterium for a 1-D ideal MHD

model, stating the result in terms of "inverse twist"; we will use his analysis to estimate the stability of our configuration when there is a detached flux tube. The stability of a 1-D ideal MHS model cannot, of course, be applied to our model in detail. However, the 1-D model does give a sufficient condition for stability of the 2-D MHS model. This is because line-tying, gravity, and the surrounding ambient plasma and magnetic field are all stabilizing effects; if the 1-D model is stable, then for the same amount of twist, our 2-D model is certainly stable as well.

According to the 1-D analysis, and therefore approximating the field structure of the detached flux tubes by a cylindrical geometry, the inverse field twist of the outermost flux tube is expressed by q, defined as:

$$q = \frac{\pi a B_x}{L B_p}$$

Here, B_p and B_x are the poloidal and axial components of the magnetic field at the top of the outermost detached flux tube, L is the tube length, and a is the diameter of the outermost detached flux tube. We assume L/a=5 based on observations of erupting filaments (Priest, 1984). The magnitude of q determines the degree of field twist; lower q means higher twist. By definition, q is the reciprocal of the number of times a field line on the flux surface (of diameter a) wraps around the tube per length L along the axis of the tube. With these definitions, Bateman (1978) shows that a cylinder is stable against kink modes

if q>1. Under the conditions in our model, this can be taken as a sufficient condition for stability.

(c) Definition of Shear Length

In our model, changing magnetic shear, or quasi-static shear motion, is simulated by changing γ for a given choice of α. However, shear is not necessarily defined simply by a value for γ (Jockers, 1976, 1978). It is therefore necessary to specify exactly how magnetic shear depends on γ. A mathematical description of the shear length, d, of a field line on a flux surface of constant potential A is given by Heyvaerts, et al. (1982):

$$d(A) = B_x(A) \int_o^{y(A)} \frac{dy}{B_y} . \qquad (14)$$

This integration is carried out along a field line on a specific flux surface, from y=0 to y=y(A) in our case. The shear length is the physical quantity in which we are interested but its dependence on γ, through the integral in (14), is nonlinear. Consequently, we will find that d(A) does not increase linearly with γ or, equivalently, the ratio $d(A)/\gamma$ depends on the value of γ. This point will be important later in the discussion of the behaviour of shear length for $\gamma > \gamma_c$.

III. QUASI-STATIC EVOLUTION

Because there are two independent parameters in our model, γ and α, there are two independent ways we can simulate quasi-static evolution corresponding to two different physical changes. Increase of axial current and helical twist is achieved through increasing α while holding γ constant. Conversely, magnetic shear is increased by increasing γ while holding α constant.

When changing the model parameters, care must be exercised to insure that the physical quantities remain within realistic bounds, particularly the plasma β. As α increases, pressure increases over the ambient hydrostatic pressure, p_o, through the dependence of $p(y,z)$ on $f(A)$ shown in (6) and, hence, on α. Therefore, increasing α tends to increase β. Conversely, increasing γ causes a decrease in β because the magnetic pressure is increased with no appreciable change in the plasma pressure. When we study the quasi-static evolution of a qiescent filament channel by increasing alpha we have to impose the constraint that β be no greater than of order unity. For the corona in the arcade over and around a quiescent filament, if we take $T=2\times10^6$k, $n=5\times10^8$ cm^{-3}, and B=5G, then β is about 0.1; in the filament itself with $T=10^4$ k, $n=10^{12}$ cm^{-3}, and B=5G, β is about 1. For our model, we have found that this constraint requires that $\gamma>6$ under changing α. In other words, the field twist cannot indefinitly increase without resulting in an unrealistically high β. For a realistic β, the magnetic field requires some shear for a given value of α. This constraint may explain the observed

"PAGE MISSING FROM AVAILABLE VERSION"

considerable shear angle in quiescent filaments. Leroy et al. (1984) found that Kippenhahn-Schluter type filaments (Kippenhahn and Schluter, 1957) have a shear angle of about 60° (30° to the neutral line) and Kuperus-Raadu type filaments (Kuperus and Raadu, 1974) have a shear angle of 65°. These observed angles agree well with the shear angle 68° in our model with $\alpha=4$ and $\gamma=6$ (Fig. 3a).

Fig. 3 shows how magnetic field changes as we increase α with $\gamma=6$. We start with sheared magnetic field with some twist ($\gamma=6$, $\alpha=4$) inside of non-sheared field. The shear angle of the field line near the neutral line is 68°. As we increase α (or axial current) to $\alpha=4.5$ a thin detached flux tube appears near the neutral line. The estimate of q using eq. (13) shows that $q=2.38$ implying that the equilibrium is stable. For $\alpha=5$ the flux tube becomes bigger and q becomes 0.6 which is less than 1, implying that the field configuration might be ideal MHD unstable. The β value at the end of this sequence is about 3 on the neutral line. Further quasi-static evolution is meaningless beyond this point because of the instability.

Fig. 4 shows quasi-static evolution of shear with γ for $\alpha=2$. The initial configuration, Fig.4(a), has a shear angle 57.6°. Until γ increases to a critical value, $\gamma=39.2$, all the field lines are rooted to the lower boundary; so each equilibrium of the sequence is MHD stable. For $\gamma=39.2$ (Fig. 4(b)), the field lines near the neutral line are highly sheared with a shear angle 87.9° and the maximum β value is about 0.3 for $\gamma=39.2$. The stability allows further quasi-static evolution over

γ=39.2. When we increase γ from 39.2 to 39.25 a discontinuous change occurs. Fig.4(c) shows a drastic change from highly sheared low lying field lines to seemingly open field lines for the increment of γ by 0.05. Since only the lower parts of the field lines are drawn, we cannot see the whole configuration. If we draw field lines projected on the y-w plane, which covers $0<z<\infty$ by the transformation of $W = e^{-\frac{\lambda}{z} z}$, we can see that there are no open field lines; all the field lines are closed (detached) or rooted in the lower boundary but highly inflated. The height of the outermost closed field line is 2.6×10^{10} cm which is more than one third of the solar radius. Magnetic energy also changes drastically. Magnetic energy built up by increasing γ is calculated per unit length in x-direction by integrating $B^2/8\pi$ all over the y-w plane and substracting the total magnetic energy for γ=0. Thus, Fig.5 shows the magnetic energy build up due to shear. The magnetic energy builds up continuously as γ increases (shear increases) up to γ=39.2, then discontinuously increases for higher γ. Other energies (internal, gravity) follow the same pattern with much smaller magnitude.

IV. QUIESCENT FILAMENT ERUPTIONS AND FILAMENT-DISRUPTION FLARES: SEPARATE MECHANISMS

Quiescent filaments have apparently stable global magnetic structure with lifetimes of several days to weeks but most of them erupt at least once in their life time. Observations show

that quiescent filaments have moderate magnetic shear, the field in the filament making an angle of 15°-30° to the neutral line (Tandberg-Hanssen and Anzer, 1970; Leroy, 1978; Nikolsky, et al., 1984; Leroy, et al. 1984). If a quiescent filament has detached field lines these lines could be twisted more than one turn from one end of the filament to the other. For a long filament, field lines could twist several turns along the filament making it susceptible to kink instability. Therefore, the Kuperus-Raadu type of configuration in which a filament forms in a detached flux tube above an x-point might not have the long term stability that observations show. A similar model by Pneuman(1983), in which a detached flux tube is formed by reconnection from an arcade field, may also be MHD unstable and hence not viable as a mechanism for filament formation. When a filament erupts, however, observations clearly show a loop structure with magnetic field lines wrapped several times around the loop. The stable nature of quiescent filaments before eruption and the twisted loop structure of an erupting filament together suggest that the initial filament field configuration is of Kippenhahn-Schluter type which develops a detached twisted tube before eruption. With what mechanism, then, does the Kippenhahn-Schluter configuration evolve to a helical configuration? The reconnection mechanism of Pneuman(1983) is a possible mechanism but it needs self-consistent MHD calculation to prove that the reconnection is dynamically possible. The mechanism we consider is the quasi-static increase of axial current and/or magnetic shear as shown in Fig. 3 and 4. A sufficient increase of the

axial current produces a detached tube with twisted field lines which is unstable to ideal MHD kink instability. Then quasi-static evolution is overtaken by instability and eruption. The eruption may not necessarily be accompanied by violent restructuring of filament field lines (in other words, a flare) because it is essentially an ideal MHD phenomenon. In this concept, the origin of the axial current is not known but may be attributed to a photospheric plasma motion.

Active regions present a different situation. Hagyard et al.(1984) found that flares occur in active regions with highly sheared magnetic field. They propose that there is a critical value of shear for the onset of a flare. Our result supports this view by showing discontinuous evolution of MHS equilibria at a critical shear. Improving on previous studies, we have modeled the quasi-static evolution of non-force-free equilibria rather than force free equilibria and have a more realistic field geometry. As shear increases in our model, axial magnetic field in the shear region increases and magnetic energy is built up in the region. Since axial magnetic field is a stabilizing effect for kink modes the quasi-static shear motion enhances the stability. Fig.4 shows that each equilibrium of the sequence is stable up to the critical point. If shear motion enhances the stability, what is the triggering mechanism of a filament disruption and flare in an active region? An attractive mechanism is the lack of an neighboring equilibrium for a shear angle over a critical value. Since the total energy(magnetic, gravity, and internal) increases discontinuously and by a large

amount across the critical point it is not likely that the equlibrium state of Fig.4(b) evolves directly to the state of Fig.4(c). The detailed dynamic processes should be studied numerically, but the following evolution might occur: Eq.(5)-(7) imply that as shear (or γ) increases, plasma current and axial magnetic field increase, causing the enhancement of plasma pressure in the force balance equation. Since plasma pressure does not directly depend on γ (see equ.7), the enhancement is not directly caused by the shear motion; the increase of shear (or γ) causes the inflation of the magnetic surfaces due to magnetic pressure build up, which, then, enhances the plasma pressure through the source term, f(A), (see equ.7). Therefore, the enhancement of plasma pressure is regarded as a response to the quasi-static increase of the Lorenz force. For an isothermal atmosphere, pressure enhancement implies density enhancement which should be supplied from chromosphere. In our quasi-static model, as $B_x(A)$ increases over a critical value the Lorenz force increases discontinuously; in the actual dynamical evolution, this may correspond to a huge force imbalance in the shear region. Hence, we identify the jump in the Lorenz force with the onset of dynamic processes including reconnection, wave generation and energy release, resulting in a flare.

V. DISCUSSION

If there is a critical shear for a flare, is the critical shear the same for all flares? Athay et al. (1985,a,b; 1986)

found that flares often occur on neutral lines with strong magnetic shear and Hα filaments. This shows that shear is both an important and common ingredient of flares. However, they observed that strong shear can be present without producing flares. Why do some high shear regions produce flares (Hagyard and Rabin, 1986) but some others do not? We suggest that depending on the magnitude of non-force-free current, some regions need higher shear than other regions for flaring. We perform quasi-static shear motions by increasing γ and calculate the critical shear length of a field line near the neutral line for various α. Fig. 6 shows that depending on α value the critical shear length varies. This result may explain why not all the high shear regions flare. There is a critical shear above which a flare is triggered but the critical value varies depending on the non-force free current in the region.

We have modeled quasi-static shear motions by increasing γ for a prescribed form of $B_x(A)$, rather than by increasing shear length at the lower boundary. Jockers (1976;1978), however, pointed out that the non-neighboring equilibrium above a critical $B_x(A)$ does not necessarily mean a solar flare. He solved a highly nonlinear force-free equation and found two solutions for a given boundary condition. As B_x increases to a critical value the two solutions merge to a critical solution, above which no solution exists. Jockers calculated shear length for equilibria near and at the critical point and found that the shear length increases from one branch to the other through the critical point. Hence, B_x increases to

the critical value as shear increases to the shear of the critical solution but decreases as shear increases over the critical shear. Jockers, then, claimed that because shear, not B_x, is the physical quantity to be prescribed, the lack of a solution above a critical B_x does not mean dramatic change in the magnetic field. The continuous increase of shear length through the critical solution only restricts the magnitude of $B_x(A)$ to the value lower than the critical value. The importance of this point is recently addressed again by Aly (1984), Low (1986), and Priest (1986).

We have solved the MHS equation, eq. 7, for given source functions, equ.(8) and (10) or equ.(9) and (10). We find the lack of an equilibrium for critical γ (or critical $B_x(A)$) for the source functions, equ. (8) and (10) but obtain the lack of a neighboring equilibrium for the source functions, equ. (9) and (10). How does the shear length change as γ increases over the critical value? Does the lack of a neighboring solution for B_x above the critical value not mean the dramatic change of the magnetic field as Jockers pointed out? Fig. 7 shows how magnetic shear changes as γ increases. Shear length d(A) of each field line designated by A at the lower boundary, which is defined in Eq.(12), is plotted for different γ. As γ increases to the critical value, shear increases and is highly concentrated near the neutral line. As γ increases over the critical value $\gamma=39.2$ to $\gamma=39.25$ the shear increases. We, therefore, believe that Jockers's argument about the critical B_x is not applicable to our configuration. In other words, it appears that there will be a

violent change of field configuration if the shear increases past the critical amount.

We have checked the stability of each equilibrium of the quasi-static evolution by applying a 1-D ideal MHD stability criterion. The stability criterion provides only an indication of instability; it is not a rigorous criterion. Gravity, photospheric line tying of field lines, and surrounding plasmas and magnetic fields, which are all stabilizing effect of a kink instability, will alter the instability criterion from the 1-D MHD criterion. A rigorous analysis of the MHD stability of our 2-D model is outside the scope of this paper. We believe, however, that the result of a full analysis would be qualitatively the same as we found in this paper.

VI. CONCLUSION

Active region filaments are in strong magnetic field regions and have high magnetic shear while quiescent filaments are in weak field regions and have moderate shear. The fundamental difference of magnetic structure leads us to propose that these two classes of filaments have different mechanisms for eruption.

The magnetic structure of a quiescent filament region can evolve to form a detached helical flux tube above the neutral line by increasing axial plasma current. If the field lines wrap more than one time around the tube from one end to the other, then the loop can erupt due to ideal MHD kink instability without

undergoing major topological change. Observations of quiescent filament eruptions (Tandberg-Hanssen, 1974; Priest, 1982) show field lines wrapping more than one time around the erupting filament. We do not, however, exclude the possibility that a quiescent filament can erupt due to the lack of a neighboring equilibrium for a filament with low aspect ratio. Since q is inversely proportional to the aspect ratio, lower aspect ratio produces higher q value for given B_x and B_p values. For aspect ratio 3, for example, the equilibrium of Fig.3(c) is stable because of q>1. If we increase α over 5, we have the lack of a neighboring equilibrium before the equilibrium becomes unstable. The lack of a neighboring equilibrium may accelerate reconnection such that a quiescent filament erupts by the mechanism proposed by Hagyard, Moore, and Emslie (1984). Such a quiescent filament eruption could well produce appreciable flare brightening in the chromosphere. Since, however, most erupting quiescent filaments have aspect ratio higher than 3 (Priest, 1982), it appears that MHD instability is the more likely mechanism.

On the other hand, an active region filament with high shear has strong axial magnetic field which stabilizes the kink instability. Our simple estimate of stability for the sequence of equilibria with increasing shear shows that the equilibria are all stable until $B_x(A)$ reaches a critical value. Magnetic energy is stored in the stable magnetic structure by shear motion. As shear increases over the critical value, a violent reconfiguration of the topology occurs, which may be interpreted as the initiation of a flare.

ACKNOWLEDGEMENT

We acknowledge support for this research provided by NAS/NRC, NASA office of Solar and Heliospheric Physics, and by the Space Plasma Physics Branch.

REFERENCES

Aly, J. J., 1985, Astron. Astrophys. 143, 19

---------- 1984, Astrophys. J., 283, 349

An, C.-H., 1982, Solar Phys., 75, 19

An, C.-H., 1984, Astrophys. J. 281, 419

Athay, R. G., Jones, H. P., and Zirin, H., 1985a, Astrophys. J., 288, 363

----------, Astrophys. J., 291, 344

----------, Astrophys. J., 303, 877

Barnes, C. W., and Sturrock, P. A., 1972, Astrophys. J., 174, 659

Bateman, G., 1978, MHD Instabilities (Cambridge: MIT Press)

Birn, J., Goldstein, H., and Schindler, K., 1978, Solar Phys. 57, 81

Canfield, R. C., Priest, E. R., and Rust, D. M., 1974 in Y. Nakagawa and D. M. Rust(eds.), Flare-related Magnetic Field Dynamics, NCAR, Boulder, USA

Einaudi, G., and Van Hoven, G., 1981, Phys. Fluids, 24, 1092

Hagyard, M. J., Smith, J. B., Teuber, D., and West, E. A., 1984, Solar Phys., 91, 115

Hagyard, M. J., Moore, R. L., and Emslie, A. G., 1984, Adv. Space Res., 4, 71

Hagyard, M. J., and Rabin, D. M., 1986, Advances in Space Research (in press)

Heyvaerts, J., Priest, E. R., and Rust, D. M., 1977, Astrophys. J., 216, 123

Heyvaerts, J., Lasry, J. M., Schatzman, M., and Witomsky, P., 1982, Astron. Astrophys. 111, 104

Hood, A. W., 1983, Solar Phys., 87, 279

Hood, A. W., and Priest, E. R., 1979, Solar Phys., 64, 303

----------, 1980, Solar Phys., 66, 113

Jockers, K., 1976, Solar Phys., 50, 405

----------, 1978, Solar Phys., 56, 37

Kawaguchi, I., 1967, Solar Phys., 1, 420

Kippenhahn, R., and Schluter, A., 1957, Zs. Ap. 43, 36

Kuperus, M., and Raadu, M. A., 1974, Astron. Astrophys., 31, 189

Leroy, J. L., 1978, Astron. Astrophys., 64, 247

Leroy, J. L., Bommier, V., Sahal-Brechot, S., 1984, Astron. Astrophys., 131, 33

Low, B. C., 1975, Astrophys. J., 197, 251

----------, 1977, Astrophys. J., 212, 234

----------, 1986, Astrophys. J., (in print)

Migliuolo, S., and Cargill, P. J., 1983, 271, 820

Nikolsky, G. M., Kim, I. S., Koutchmy, S., and Stellmacher, G., 1984, Astron. Astrophys., 140, 112

Pneuman, G. W., 1983, Solar Phys. 88, 219

Priest, E. R., and Milne, A. M., 1980, Solar Phys., 65, 315

Priest, E. R., 1984, Solar Magnetohydrodynamics (D. Reidel, Dordrecht, Holland)

----------, 1986, Solar Phys., 104, 1

Raadu, M. A., 1972, Solar Phys., 22, 425

Ray, A., and Van Hoven, G., 1982, Solar Phys., 79, 353

Roy, S.-R., and Tang, F., 1975, Solar Phys., 42, 425

Saito, K., and Tandberg-Hanssen, E., 1973, Solar Phys. 31, 105

Sakurai, T., 1976, Publ. Astron. Soc. Japan, 28, 177

Svestka, Z., 1976, Solar Flares, Dordrecht: Reidel, p 229

Tandberg-Hanssen, E., and Anzer, U., 1970, Solar Phys., 15, 158

Tandberg-Hanssen, 1974, Solar Prominences, (D. Reidel, Dordrecht, Holland)

Waldmeier, M., 1970, Solar Phys., 15, 167

Withbroe, G. L., and Noyes, R. W., 1977, Ann. Rev. Astron. Astrophys. 15, 363

Yang, W. H., Sturrock, P. A., and Antiochos, S. K., 1985 (Stanford Univ. Preprint)

Zweibel, G. W., and Hundhausen, A. J., 1982, Solar Phys., 76, 261

FIGURE CAPTIONS

Fig. 1: The coordinate system used in this paper with axial ($\vec{j}_x$) and poloidal current ($\vec{j}_p$) specified in y-z plane and the 3-D resultant magnetic field lines. $\vec{j}_p$ is distributed between Ac<A<1 and $\vec{j}_x$ is everywhere on y>0. Gravity is in negative z-direction. The field configuration is the MHS solution for γ=6 and α=4.

Fig. 2: Schematic representation of the displacement (d(A)) of the foot points of a field line on the flux surface A.

Fig. 3: Quasi-static evolution of a MHS equilibrium with increasing α (or axial current) for γ =6. T=2x10^6 k, n=5x10^9 cm^{-3}, and β=0.1 at the lower boundary.
(a) α=4; all the field lines are rooted at the lower boundary. The shear angle is θ=68°.
(b) α=4.5; a detached flux tube is now present, imbedded in sheared field lines. The flux tube is stable (q=2.4).
(c) α=5; the detached flux tube is bigger and has q=0.6. The value of q less than 1 suggest that the flux tube is kink unstable. The plasma has β=3 at y=0 on the lower boundary.

Fig. 4: Quasi-static evolution with increasing γ (increasing shear) for α=2. T=2x10^{6}k, n=5x10^9 cm^{-3}, and β=0.001 on the lower boundary at y=D/2.
(a) γ=15; all the field lines are rooted to the lower boundary. The shear angle of the field lines near the neutral line is 57.6°.

(b) γ=39.2; field lines near the neutral line are highly sheared with shear angle 87.9°. Since all the field lines are rooted to the lower boundary the field configuration is stable even though it is near the critical point. On the lower boundary, β=0.3 at x=0.

(c) A discontinuous change of field configuration with $\gamma \approx 39.25$. For clarity of the figure, the field lines are plotted only on the y>0 side of the neutral line. The field lines look open in this figure but they are closed at the height above one third of the solar radius.

Fig. 5: Magnetic energy build up by the quasi-static shear motion (increasing γ) of Fig. 4. The energy is calculated in CGS unit per length over the entire computational y-z space.

Fig. 6: Critical shear length of a field line near the neutral line v.s. the non-force free parameter α for $T=2\times10^6$ k, $n=5\times10^9$ cm^{-3}, and β=0.001 at x=D/2 on the lower boundary. The figure shows that there is a critical shear above which a flare is triggered but the critical value varies depending on the non-force free current.

Fig. 7: Shear length d(A) near the neutral line for different γ value for the case of Figure 4. Note that the shear length increases as γ increases over the critical value, 39.2.

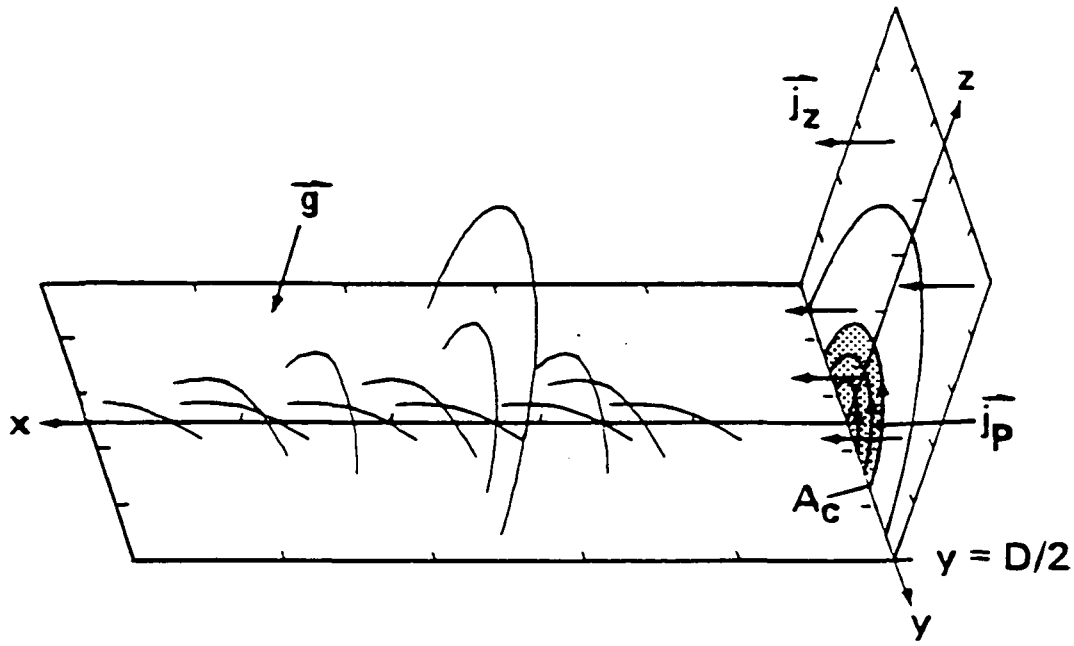

Fig.1

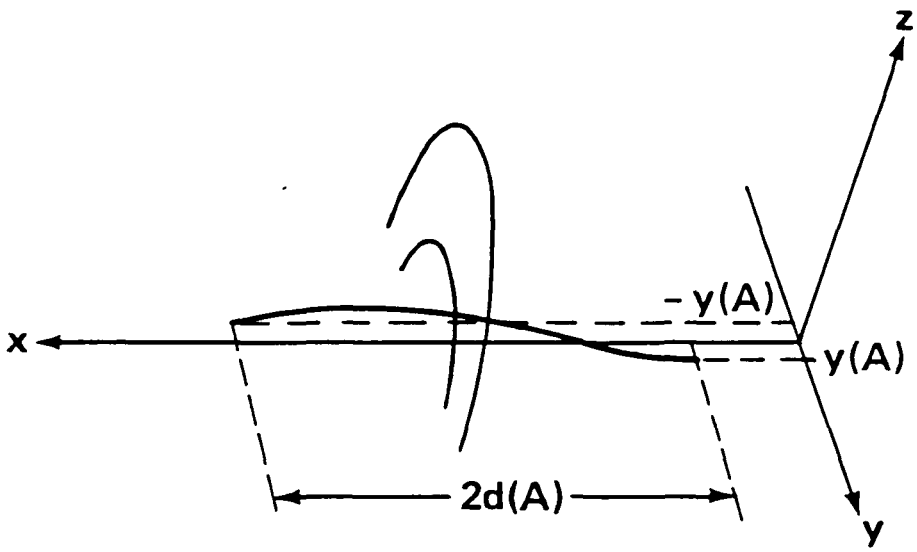

Fig.2

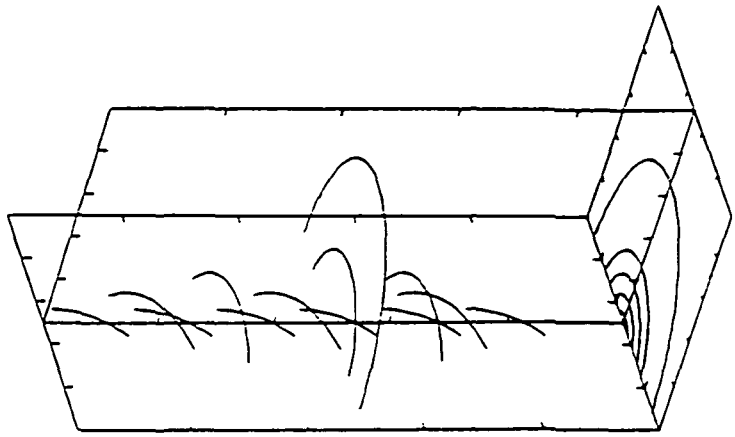

(a)

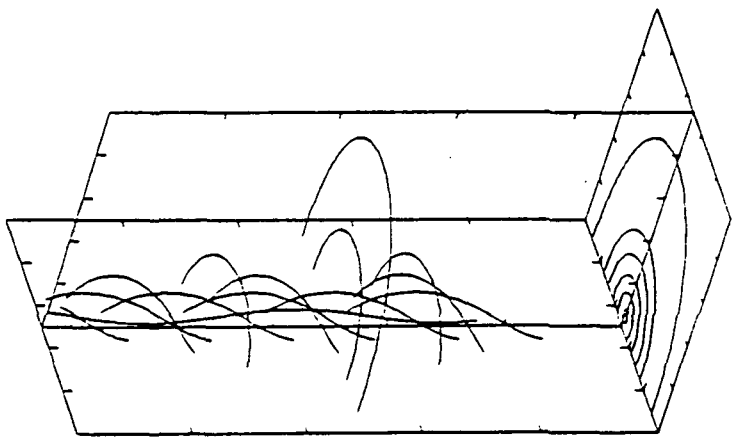

(b)

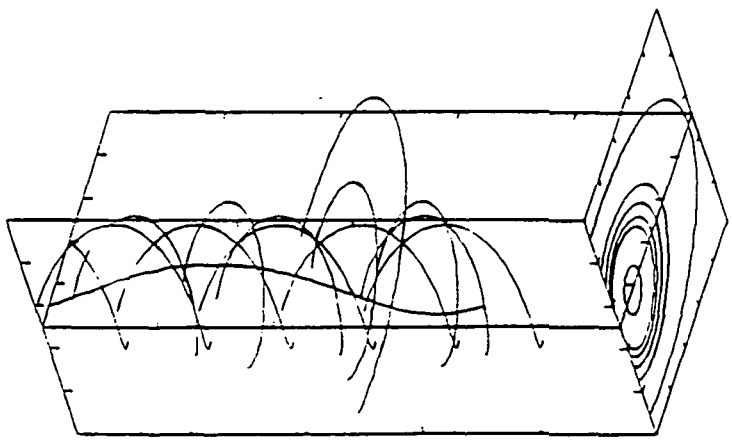

(c)

Fig.3

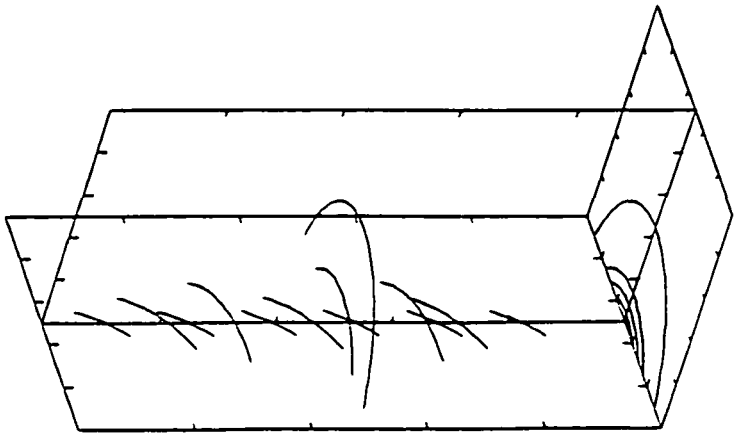

(a)

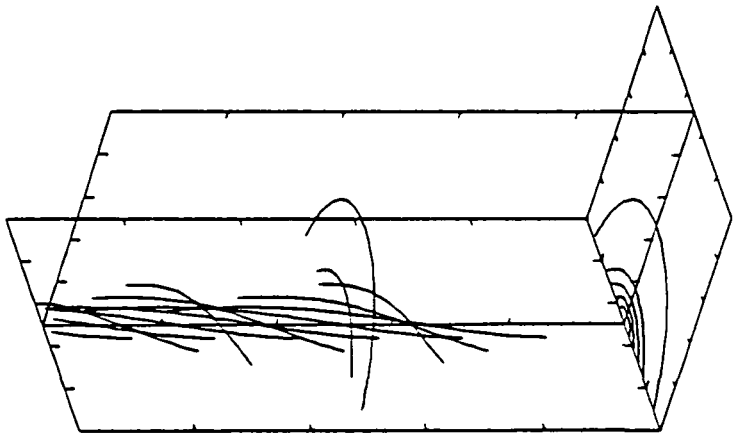

(b)

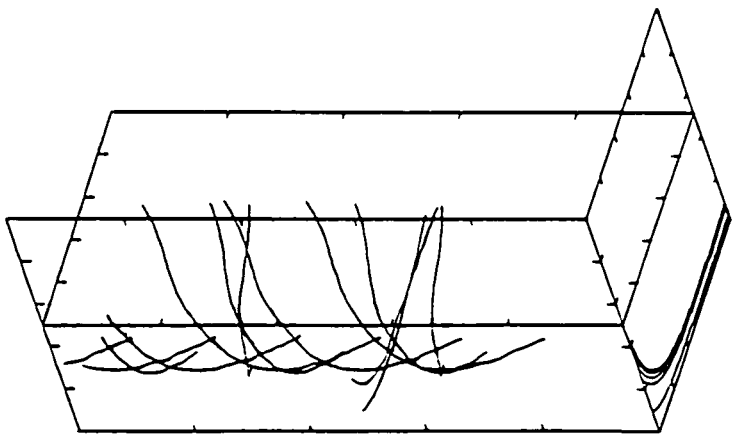

(c)

Fig.4

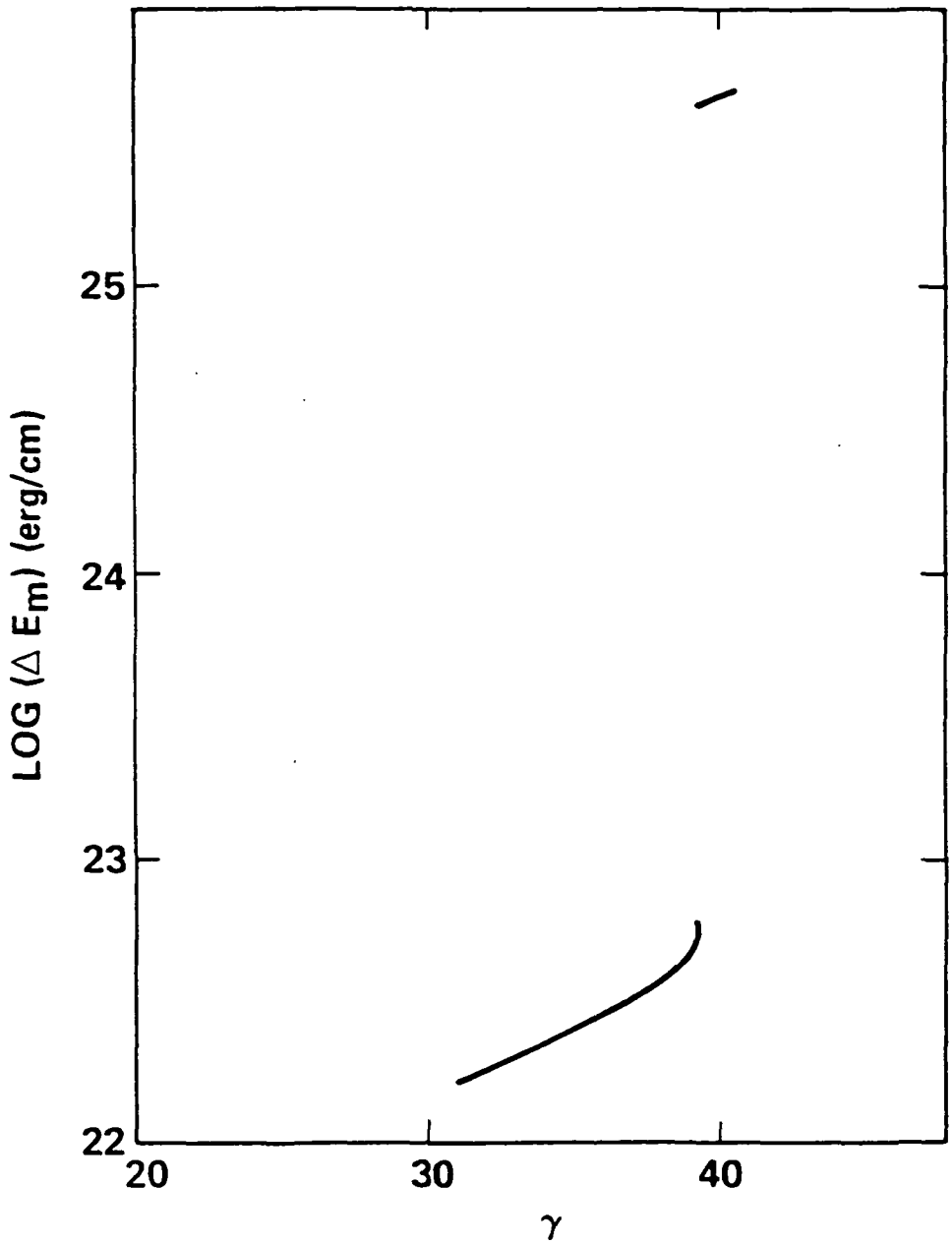

Fig.5

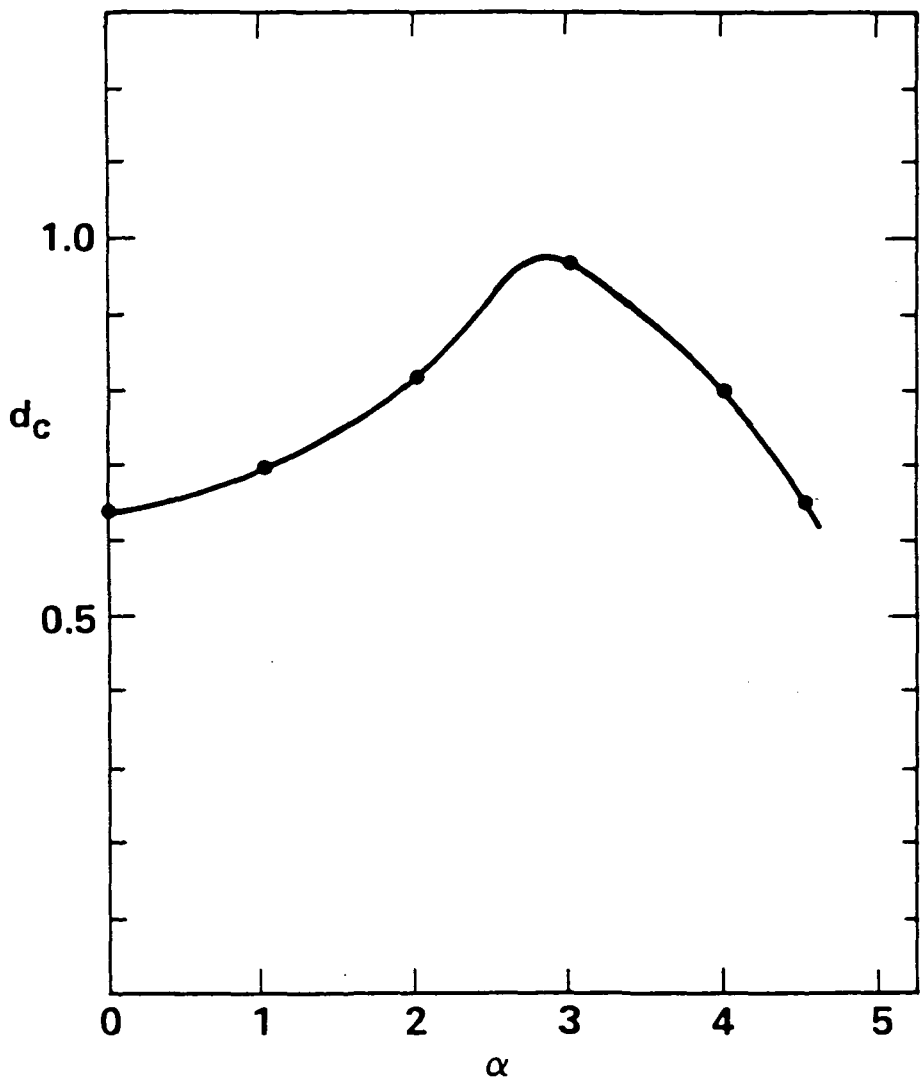

Fig.6

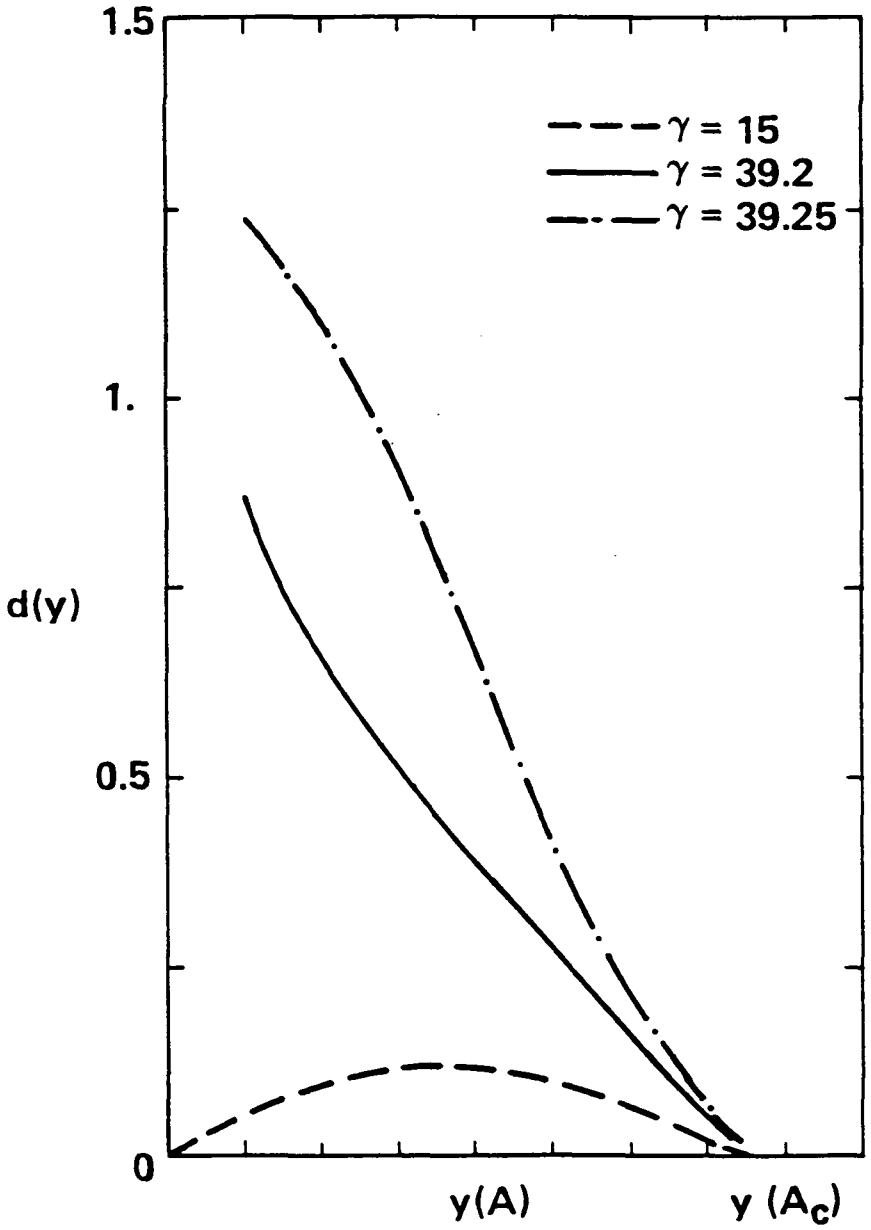

Fig.7